Journal of Alloys and Compounds 505 (2010) 801–807

Contents lists available at ScienceDirect

Journal of Alloys and Compounds

journal homepage: www.elsevier.com/locate/jallcom

Influence of processing medium on frictional wear properties of ball bearing steel prepared by laser surface melting coupled with bionic principles

Hong Zhou[a,*], Chengtao Wang[a,f], Qingchun Guo[a,g], Jiaxiang Yu[a], Mingxing Wang[b], Xunlong Liao[c], Yu Zhao[d], Luquan Ren[e]

[a] The Key Lab of Automobile Materials, The Ministry of Education, Jilin University, Changchun 130025, PR China
[b] The State Key Laboratory of Nonlinear Mechanics, Institute of Mechanics, Chinese Academy of Sciences, 15 Beisihuanxi Road, Beijing 100190, PR China
[c] Technical Management Department, CNNC China Zhongyuan Engineering Corp. Ltd., No 487 Tianlin Road, Shanghai 200233, PR China
[d] School of Materials Science and Engineering, Changchun University of Technology, Changchun 130012, PR China
[e] The Key Lab of Terrain Machinery Bionics Engineering, The Ministry of Education, Jilin University, Changchun 130025, PR China
[f] Faw-Volkswagen Automotive Company Ltd., Changchun 130011, PR China
[g] Brilliance Automobile Engineering Research Institute, Shenyang 110141, PR China

ARTICLE INFO

Article history:
Received 3 August 2009
Accepted 24 June 2010
Available online 3 July 2010

Keywords:
Ball bearing steel
Biomimetic
Laser surface melting
Microstructure
Microhardness
Wear behavior

ABSTRACT

Coupling with bionic principles, an attempt to improve the wear resistance of ball bearing steel (GCr15) with biomimetic units on the surface was made using a pulsed Nd: YAG laser. Air and water film was employed as processing medium, respectively. The microstructures of biomimeitc units were examined by scanning electron microscope and X-ray diffraction was used to describe the microstructure and identify the phases as functions of different mediums as well as water film with different thicknesses. The results indicated that the microstructure zones in the biomimetic specimens processed with water film were more refined and had better wear resistance increased by 55.8% in comparison with that processed in air; a significant improvement in microhardness was achieved by laser surface melting. The application of water film provided considerable microstructural changes and much more regular grain shape in biomimetic units, which played a key role in improving the wear resistance of ball bearing steel.

1. Introduction

Ball bearing steel in hardened and tempered condition with predominantly tempered-martensitic microstructures is the most widely used material for ball bearing applications, practical precision measuring implements, cold punching dies and lead screws of machine tools. The universal popularity of this steel in the above applications arises from the attractive combination of low cost, high yield/tensile strength, and good machinability and formability [1]. However, this steel, with relative motion between interacting surfaces, is required to run smoothly under severe operating conditions such as larger contact loads, higher speeds, or even higher temperatures. Furthermore, contact fatigue and frictional wear are found to be inadequate at times in heavy duty/load applications. These situations put forward higher demands for properties of this steel, and it was suggested that protecting the steel with an excellent wear resistance layer was an adequate solution to improve these properties, without change of the advantageous bulk properties. Over the past two decades, in order to improve surface properties of this steel, scientific work was carried out at home and abroad [2–9]. These results which had led to some achievements in surface treatments were widely employed due to their scientific, technological and industrial applications. As one of the new and effective treatments, laser surface melting, associated with subsequent rapid resolidification, is a means of producing a refined or metastable microstructure in localized areas on a component, which have improved service properties such as resistance to wear, corrosion and oxidation, particularly at high temperatures. Up to recent, it was applied to improve surface properties of materials [10] and previous results showed that a wide variety of surface properties could be significantly improved with reasonable process parameters [11–23].

Bionics is a science that imitates the principles of bio-systems to build new technological systems for useful components. Over the past two decades, bionics had been attracted considerable attention on material science and engineering, because the unique structures, compositions and correspondingly excellent properties of biology gave researchers many clues to improve the properties of materials or increase the reliability of structural components [24]. The Lotus effect verified by Neinhuis and Barthlott [25] was applied to the study of water-repellent or anti-adhesive materials and resulted directly in the invention of anti-adhesive ceramic tile

* Corresponding author. Tel.: +86 431 85094427; fax: +86 431 85095592.
E-mail address: wangct08@mails.jlu.edu.cn (H. Zhou).

0925-8388/$ – see front matter © 2010 Elsevier B.V. All rights reserved.
doi:10.1016/j.jallcom.2010.06.144

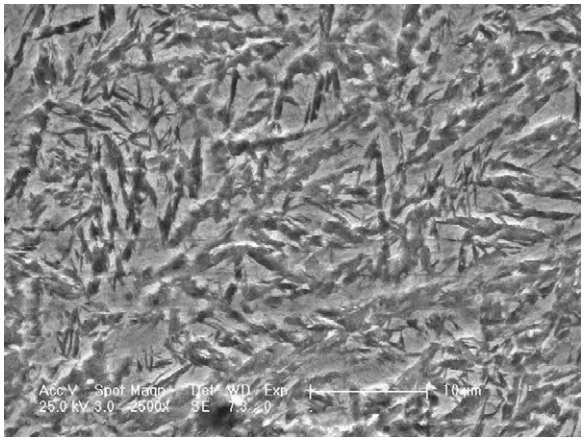

Fig. 1. The original microstructure of the substrate.

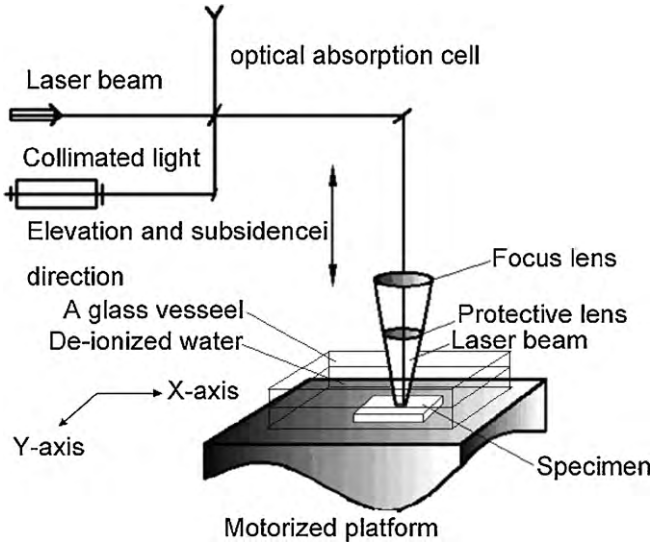

Fig. 4. The schematic diagram of the experimental setup for laser surface melting under water film.

on the wall; a biomimetic process for coating an apatite layer on many types of materials was developed by Kokubo and co-workers [26,27], and so on. Ren et al. [28–30] have been dedicating to the study of the cuticle morphologies and principles of soil animals such as dung beetles, black ants, and pangolins and found that there were generally five kinds of simple structures on the cuticles, including convex, concave, stria, bristle and squama. These so-called non-smooth construction units have been found to provide excellent anti-wear properties against soil. Recent works in our research group also found that there was a considerable effect on both improving the abrasive wear and thermal fatigue resistance when biomimetic principle was applied on the cast iron, die and tool steel surfaces to form a series of biomimetic units by laser surface melting [24,31–36]. Based on the results mentioned above, we concluded this study to explore whether similar benefits could be obtained to improve wear resistance of GCr15 bearing steel processed by laser surface melting coupling with bionic principle with different processing medium, without changing the special properties of substrate materials.

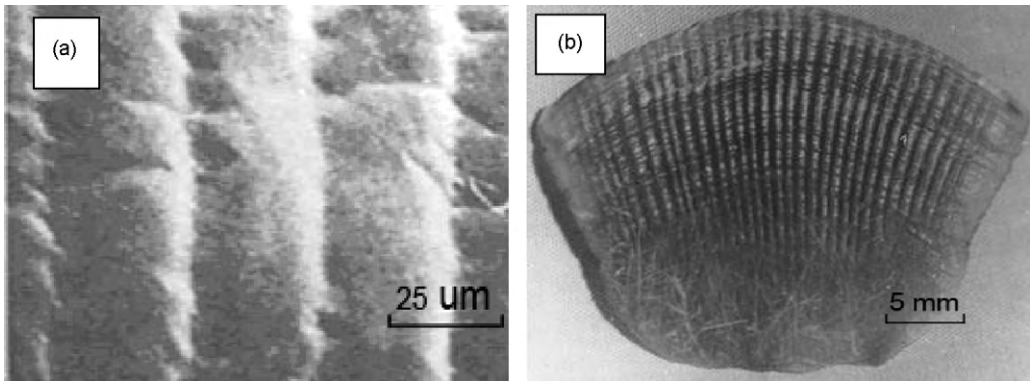

Fig. 2. SEM and OM micrograph of typical shape of body surface of soil animals: (a) stria shape of elytron and (b) striate non-smooth surface on the squama of pangolin.

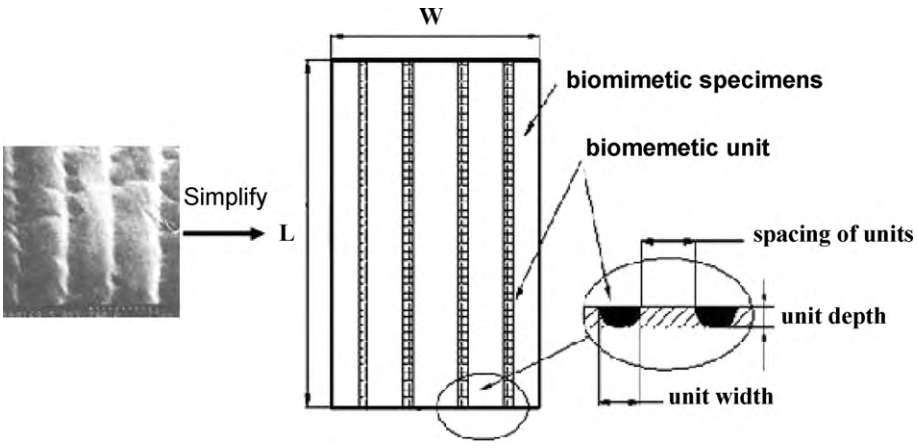

Fig. 3. Model simplification of biomimetic specimen.

Table 1
Chemical compositions of GCr15 bearing steel (wt.%).

C	Si	Mn	Cr	P	S	Fe
0.950–1.050	0.150–0.350	0.200–0.400	1.300–1.650	<0.027	<0.020	Remainder

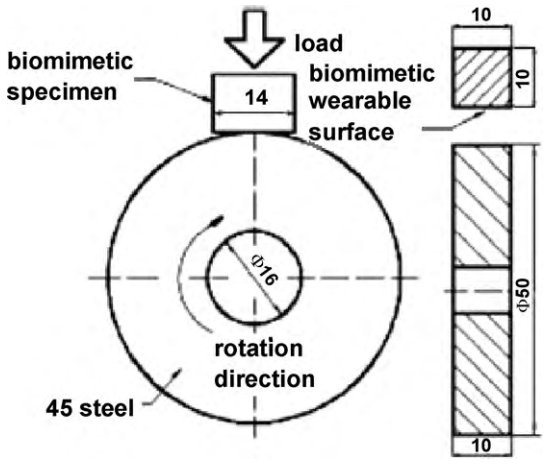

Fig. 5. The schematic illustration of the block-on-ring wear tester.

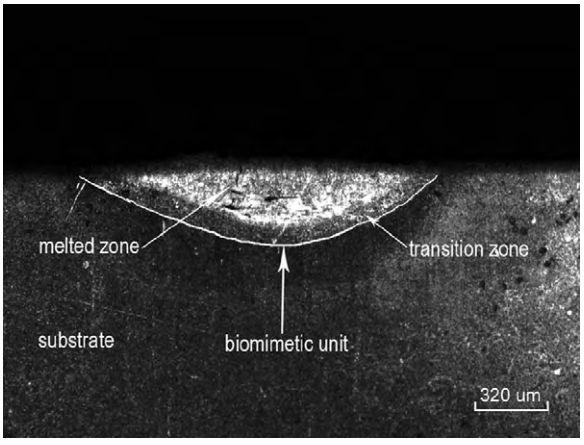

Fig. 6. Optical micrograph of biomimetic unit obtained by laser surface melting in water film.

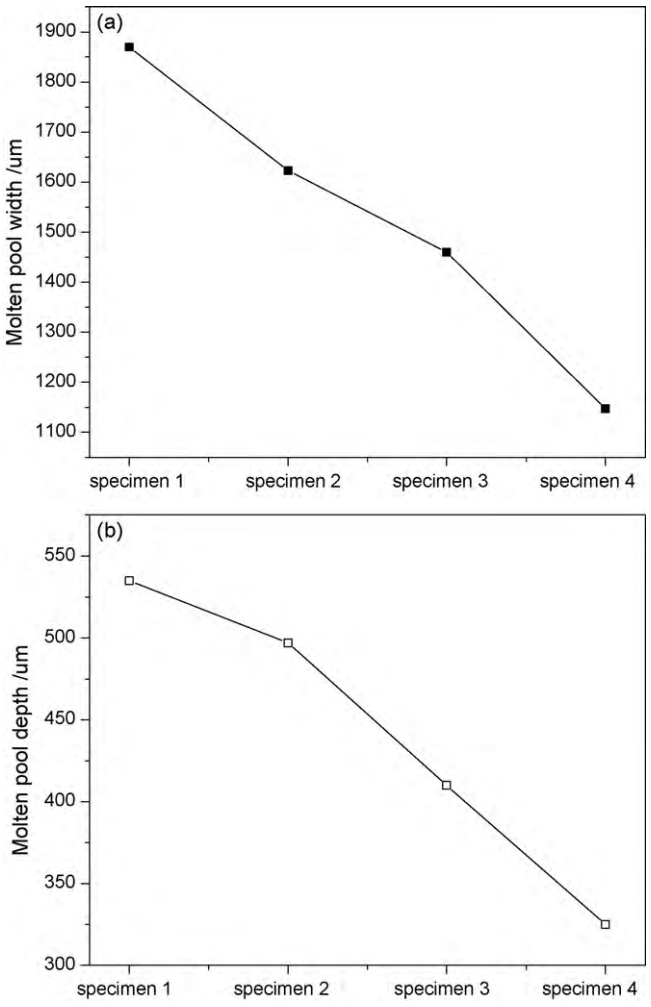

Fig. 7. Molten pool parameters of biomimetic specimens.

In the present study, we chose the laser facility to manufacture and process biomimetic units on the surface of GCr15 bearing steel and to form a novel bio-inspired wearable surface. Wear tests were carried out on a block – on ring with a biomimetic GCr15 block against a 45 steel ring. Experiments were focused on the effects of medium and thickness of water film on the wear behavior of the bio-inspired wearable surface under dry sliding condition.

2. Experimental

2.1. Materials

GCr15 (ball bearing steel) is in Chinese standard of YB9 and similar to AISI 52100 in USA standard. Specimens of the steel in a quenched and tempered state were investigated. Chemical compositions of GCr15 ball bearing steel are given in Table 1. Fig. 1 shows the original microstructure of substrate, which had an acicular martensitic microstructure. All specimens were polished to a surface roughness, Ra, of 0.04 μm, flat and smooth specimens of size with 14 mm × 10 mm × 10 mm.

2.2. Preparation of biomimetic specimens

Mimicking the cuticles of dung beetles [37] (Fig. 2), various stria biomimetic units were processed by laser beam using a pulsed Nd: YAG laser in a pulse wave mode, operating at 1064 nm, maximum power 300 W with a Gaussian distribution of the energy in the beam. A schematic illustration of biomimetic specimens is shown in Fig. 3. The space between two neighboring traces on biomimetic specimens is 2 mm. Fig. 4 is a schematic diagram of the laser surface melting apparatus. Air and de-ionized water was used as processing medium, respectively. A series of experiments

Table 2
Parameters of specimens and medium in different thicknesses.

No.	Specimen size	Spacing of units	Medium	Thickness
1	14 mm × 10 mm × 10 mm	2 mm	Air	–
2	14 mm × 10 mm × 10 mm	2 mm	De-ionized water	1 mm
3	14 mm × 10 mm × 10 mm	2 mm	De-ionized water	2 mm
4	14 mm × 10 mm × 10 mm	2 mm	De-ionized water	3 mm

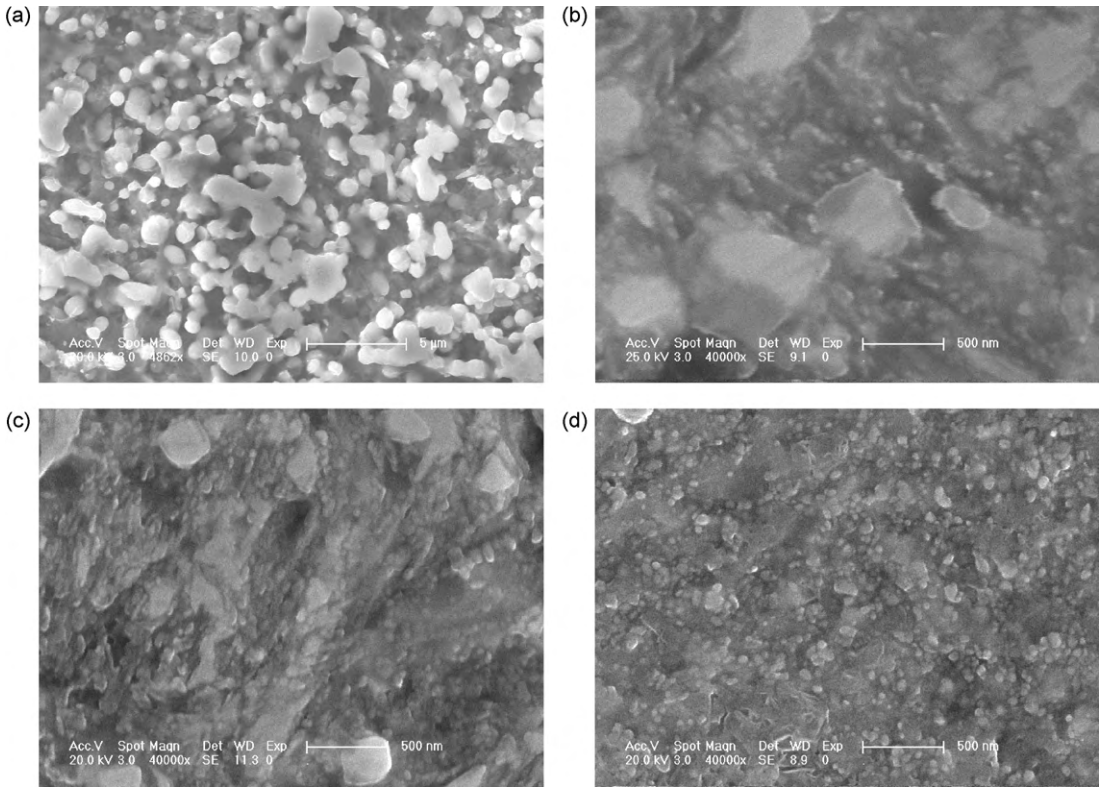

Fig. 8. Field-emission scanning micrographs (FESEM) structures of the melted zone of the biomimetic specimen processed in air (a) and with water film with various thicknesses: (b) 1 mm, (c) 2 mm, and (d) 3 mm.

were carried out in air and water film in thickness of 1, 2 and 3 mm when all the laser input energies were 160 J/cm^2 to form the stria biomimetic units on the surfaces of specimens to investigate the influence of the thickness of medium on the wear resistance. The processing parameters were a duration pulse of 5.0 ms, a frequency of 3 Hz, a beam diameter of 50 μm, a defocusing amount of 5 mm and a scanning speed of 0.71 mm/s. Table 2 shows the parameters of specimens.

After the laser processing, transverse sections were obtained and the standard method of metallography was followed to prepare the specimens for the microstructure analysis and the microhardness measurement, using a JSM-5600LV scanning electron microscope and a Vickers Microhardness Tester (model 5104, manufactured by Buehler Co. Ltd., USA) with a 25-g applied load. A laser confocal scanning microscope (OLYMPUS LEST-OLS3000) was used to analyze the details of biomimetic units and wear behavior. Molten phase structures were identified by X-ray diffraction (D/max-1200 X-ray diffraction). The Cu Ka radiation at 40 kV with a current of 40 mA was used as the X-ray source and the detector scanned the samples with an angle of 0.02°.

2.3. Wear tests

Dry sliding wear tests were performed using an MM-200 block-on-ring wear tester (made by the Xuanhua Testing Machine Factory) at room temperature. Fig. 5 shows its schematic diagram. A stationary GCr15 block slid on a rotating 45 steel in quenched and tempered state, which had an average hardness of 600 HV with size of 16 mm × 50 mm × 10 mm (inside diameter × outside diameter × thickness). A normal load of 8 kg was used for wear tests. The rotational speed of the ring was 400 rpm and the sliding time was 30 min. Before each test, the surface of the steel ring was polished to a roughness of about 0.1 mm, while biomimetic specimens were ultrasonically cleaned in anhydrous alcohol and dried before and after wear tests. The mass loss was measured by a sensitive electronic balance with an accuracy of 0.0001 g. The differences in average mass loss among the four test blocks before and after the experiment were measured and accounted.

3. Results and discussion

3.1. Effect of the biomimetc unit shape and area

After the laser surface melting, a modified layer called biomimetic units was obtained (Fig. 6), which consisted of two characteristic microstructure zones, i.e. a melted zone and a transition zone. The biomimetic unit exhibited low porosity and few imperfections, and had a sound metallurgical bond with the substrate. Marangoni flow was the dominant convection mechanism in a laser-melted pool [38]. In this work, the cross-section of biomimetic units which were formed under force of Marangoni convection resulted from absorbed and dissolved O_2 [39] in the molten pool were wide shallow shape with a parabolic profile. Fig. 7 shows the effect of processing medium on both of the penetration depth and weld width. Along with water film thickness increasing, both the molten pool widths and that of depths decrease.

The mechanism can be interpreted as follows. The absorption of water to laser beam increases as water film thickness increasing from No. 2 to No. 4 when specimens were melted by laser beam, meanwhile, water vaporized immediately, and then laser beam energy that had not been absorbed was transferred through water and towards internal specimens. With high speed of energy transmission, the less energy that water film had absorbed was, the larger the unit area was. In addition, Marangoni flow plays an important role in the shape of molted pool as well. With water film thickness increasing, Marangoni convection is much stronger due to more absorbed and dissolved O_2 that generated under the irradiation of laser beam, so the Marangoni effect must be higher in the melted pool which results in a wider, shallower melted pool.

3.2. Microstructure of melted zone

Fig. 8 shows a series of SEM micrographs of the biomimetic units processed by laser beam using a power intensity of 160 J/cm^2 in air and with water film with various thicknesses of 1, 2 and 3 mm, respectively. Compared with the units processed in air, the microstructure of units processed in water film is much more refined. With water film thickness increasing, the cooling rate accelerates and crystal grain becomes refined and larger spherical particles in random locations were substituted by much more

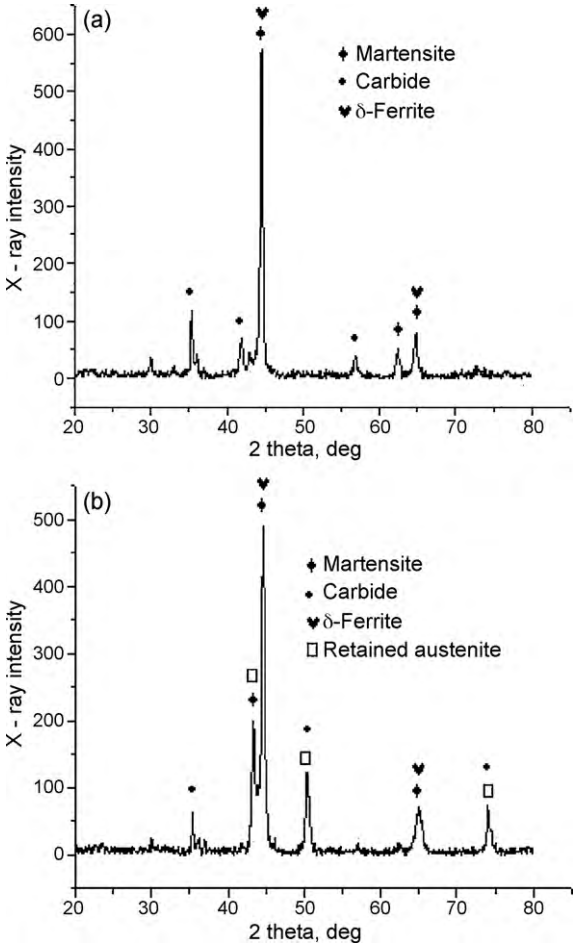

Fig. 9. . X-ray diffraction line profiles of specimens: (a) remelted in air and (b) remetled in water film.

refined microstructure gradually. The high cooling rate results in a fine solidified microstructure, which contain non-equilibrium phases and precipitates. According to XRD (Fig. 9) analysis of the melted layer, it is found that the melted zone of specimen processed in air is composed of auto-tempered martensite containing carbide and a small amount of ferrite, while that of specimen processed in water film is composed of fine martensite, a small amount of retained austenite, carbide particles and ferrite also. In addition, the X-ray spectrum (Fig. 9(b)) of specimen processed in water film exhibits a significant broadening of the peaks due to the refinement of microstructure and highly refined martensite which is of particular importance for wear resistance.

It can be interpreted as follows: The surface of the biomimetic specimen melts rapidly after laser irradiation since the melting occurs only at the surface over a relatively short duration and the bulk of the substrate remains cool, the liquid metal in the molten pool will solidify and recrystallize at a high cooling rate from which is resulted water film. At the beginning of solidification, the primary austenite forms and then crystallizes in the direction towards the surface, which corresponds to the contrary direction of the heat transfer. The last liquid will be enriched in carbon and form carbides surrounding the austenite dendrites in the fusion zone. When the temperature reaches the eutectoid point, the eutectoid reaction occurs. The solidification structures are the primary austenite and the carbides. On further cooling, there is insufficient time for the ultra-fine primary austenite and eutectoid austenite to grow, so austenite will mostly transform to martensite with some residual austenite due to extremely high cooling rates, while the primary

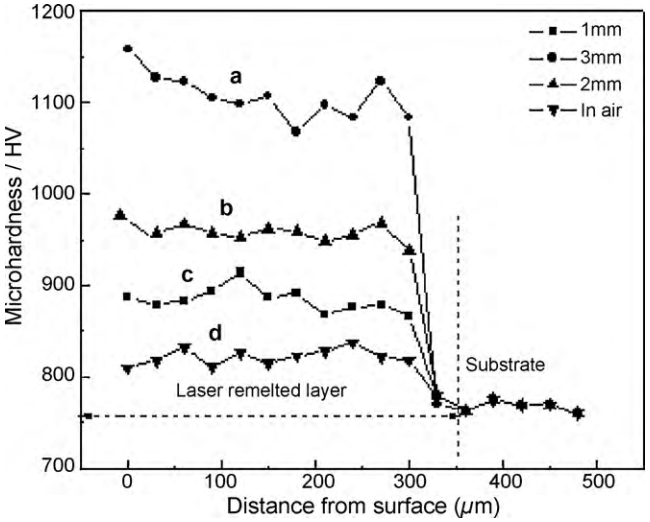

Fig. 10. Microhardness vs. distance to surface after laser surface melting under different mediums (error = ±25 HV 0.1).

carbides that have not dissolved into the primary austenite remain as carbides. Meanwhile, when water film was exploited as processing medium, molten steel has a higher Marangoni number due to more absorbed and dissolved O_2, and the Marangoni effect will be higher, which aids homogenization by convection during the solidification process. As a result, the final structure of the melted zone is fine-grained martensite, δ-ferrite, carbides and a small amount of residual austenite.

3.3. Microhardness

The results presented in Fig. 10 give an overview on the course of microhardness vs. distance top of biomimetic units processed by laser surface melting. The microhardness profiles show the typical plateau corresponding to a melted zone and a transition zone in which the hardness steeply decreases to that of the substrate. It is noted that the microhardness of specimens processed by laser beam under water film is considerably harder than that of specimens processed in air and the substrate (760 HV). The hardness of the top layer of the biomimetic units varies from 1083 to 1127 HV and the values for the top layers after laser surface remelting agreed well with Hahn et al. [40] findings. It was shown that

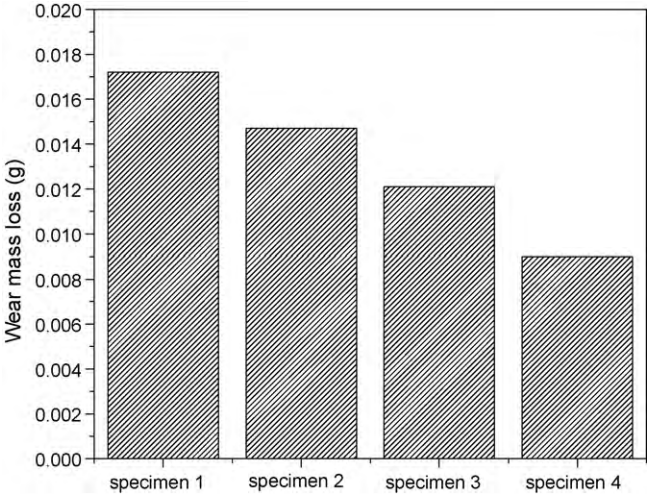

Fig. 11. . Wear mass loss of specimens as functions of gain size and bionic structure.

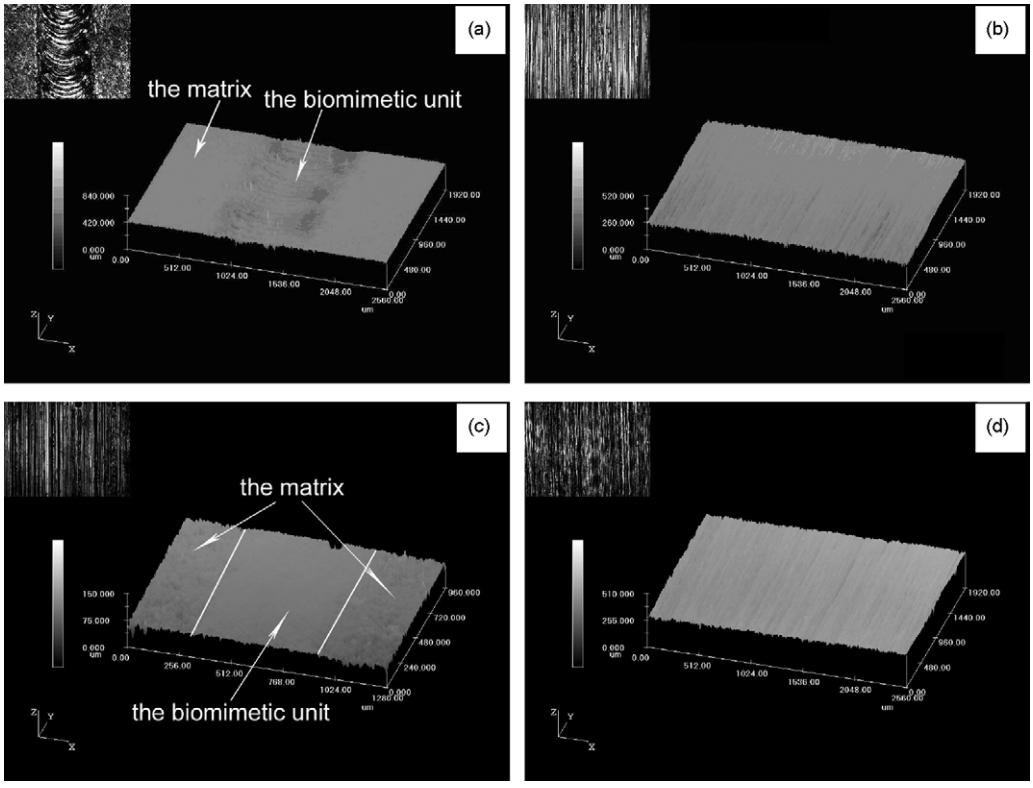

Fig. 12. The schematic drawing of wear process between biomimetic units and friction pairs.

ultra-fined microstructures have a profound effect on the microhardness. Here, the increased microhardness could be attributed to the biomimetic units which possessed some hard phases such as martensite and carbides as well, because martensite and carbide phases are mechanically the hardest while the retained austenite the softest among the various phases of the multi-phase systems. Consequently, it was concluded that such higher microhardness are mainly due to the ultra-fine martensite and the dispersion of carbides obtained by the laser surface remelting when the biomimetic units were under cooling by water film.

3.4. Wear resistance

The wear resistance specimens are divided into four groups. One group was processed in air, while the others were processed in water film with various thicknesses. Three specimens of each group were chosen for wear tests. Fig. 11 shows the variation of weight loss as functions of water film applied a load of 8 kg in 30 sliding minutes. It can be seen that the wear loss processed with different thicknesses of water film decreases by 19.5, 34.2 and 55.8%, respectively. It is noticeable that wear mass loss of specimen 4 was lowest among that of all others. The presence of ultra-fined microstructures at the surface of units imparts a beneficial effect on friction properties. We suppose that the main reason for high wear resistance of substrates lies in the effect of grain refinement, increased hardness and reinforced phases (martensite and carbides). Based on the experimental results, wear resistance of the specimens processed with water film in fact can be improved considerably under the same sliding way against the steel blocks.

3.5. Wear process and mechanism

Fig. 12 shows schematically the wear process and wear surface of biomimetic units under a normal load of 8 kg. In the wear process, the Initial wear processing takes place between the matrix and friction pairs while the concave biomimetic units are free from frictional wear as shown in Fig. 12(a). Fig. 12(b) shows a further wear process where the biomimetic units and freshly exposed surface are situated in the same plane when the salient matrix is grinded away. With the sliding time increase, the increased strength phases/hardness units with ultra-fined microstructures are hard to grind off under dry sliding wear condition. As a consequence, it indicates that wear ratio between units and frictional pairs are much lower than that of substrates, and the frictional pairs will be supported by the remaining biomimetic units (Fig. 12(c)) when the substrate among the units is grinded away. Finally, the biomimetic units will be flush with the substrate once again when all the salient units are grinded off (Fig. 12(d)). And this procedure is repeated for heaps of times to increase rubbing intensity until all the units are grinded away. As frictional pairs – biomimetic units account for an overwhelming majority in frictional system, performance of biomimetic units directly determine the wear resistance. The more the intensified biomimetic units are, the better the wear resistance of the specimens is.

4. Conclusions

The present study shows that processing medium play a positive role in improving the wear resistance of the ball bearing steel. The important conclusions emerging out of this study are the following.

1. After the laser surface melting when water film is used for processing medium, there are two microstructure zones in the biomimetic unit: the melted zone and the transition zone. Along with water film thickness increasing, both the molten pool widths and that of depths decrease resulted from Marangoni convection, which is caused by absorbed and dissolved O_2 that generated under the irradiation of laser beam.

2. An ultra-fined homogeneous microstructure (martensite + carbides) with residual austenite is achieved in the melted zone. Compared with microstructure zones of the biomimetic unit processed in air, that of the biomimetic units processed in water film are much more refined.
3. The microhardness of the melted zone increased to 1100 HV due to ultra-fined microstructures and strengthening phases in compared to 830 HV of specimens melted in air. The results show that laser surface melting with water film increases microhardness of ball bearing steel significantly.
4. Wear tests show that the wear resistance of biomimetic units against the 45 steel rings under dry sliding condition is significantly improved due to ultra-fined microstructure, increased hardness and strengthening phases. Concerning the biomimetic units, these intensified units decrease the contact area of the sliding pairs so that the wear rate reduces. In addition, along with the increase of water film, a maximum wear resistance of biomimetic units was achieved when laser surface melting was carried out in water film in thickness of 3 mm. Therefore, it is concluded that water film plays an active role in laser surface melting improving the wear resistance of ball bearing steel compared to biomimetic units processed in air.

Acknowledgements

This article was supported by the Project 985-Automotive Engineering of Jilin University, the National Natural Science Fund of China (No. 50635030) and the Science and Development Foundation of Jilin (No. 20060196) for financial support.

References

[1] H. Burrier Jr., ASM Handbook (1), ASM International, Materials Park, OH, 1997, pp. 380–388.
[2] B.Y. Tang, Y.H. Wang, L.P. Wang, X.F. Wang, H.X. Liu, Y.H. Yu, T. Sun, Surf. Coat. Technol. 86 (2004) 153–156.
[3] Q.F. Zeng, G.N. Dong, Y.B. Xie, Appl. Surf. Sci. 254 (2008) 2425–2430.
[4] F.C. Akbasoglu, D.V. Edmonds, Metall. Trans. 21A (1990) 889.
[5] T. Sun, L.P. Wang, Y.H. Yu, Y.H. Wang, X.F. Wang, B.Y. Tang, Surf. Coat. Technol. 201 (2007) 6615–6618.
[6] X.L. Liu, D.H. Wen, Z.J. Li, L. Xiao, F.G. Yan, J. Mater, Process Technol. 129 (2002) 217–221.
[7] Y.F. Lian, Q.J. Xue, H.Q. Wang, Surf. Coat. Technol. 73 (1995) 98–104.
[8] C.X. Yue, L.W. Zhang, S.l. Liao, J.B. Pei, H.J. Gao, Y.W. Jia, X.J. Lian, Mater. Sci. Eng. A 499 (2009) 177–181.
[9] P.X. Yan, S.Z. Yang, Appl. Surf. Sci. 90 (1995) 149–153.
[10] H.C. Man, Z.D. Cui, T.M. Yue, F.T. Cheng, Mater. Sci. Eng. A 355 (2003) 167–173.
[11] J. Hu, G. Liu, L.C. Kong, W.D. Fei, Appl. Surf. Sci. 253 (2006) 2792.
[12] H.C. Man, S. Zhang, F.T. Cheng, T.M. Yue, Scr. Mater. 46 (3) (2002) 229.
[13] S. Tomida, K. Nakata, S. Saji, T. Kubo, Surf. Coat. Technol. 142–144 (2001) 585–589.
[14] S.K. Putatunda, M. Nambiar, N. Clark, Surf. Eng. 13 (1997) 407–414.
[15] A.J. Hick, Heat Treat. Met. 10 (1983) 3–11.
[16] M.F. Ashby, K.E. Easterling, Acta Metall. 32 (1984) 1935–1948.
[17] W.B. Li, K.E. Easterling, M.F. Ashby, Acta Metall. 34 (1986) 1533–1543.
[18] H.B. Singh, S.M. Copley, M. Bass, Metall. Trans. A 12 A (1981) 138–140.
[19] P. Merrien, H.P. Lieurade, M. Theobalt, Surf. Eng. 8 (1992) 61–65.
[20] X.M. Zhang, H.C. Man, Li.F H.D., J. Mater. Process Technol. 69 (1997) 162–166.
[21] W.B. Li, K.E. Easterling, Surf. Eng. 2 (1986) 43–48.
[22] T. Miokovic′, Analyse des Umwandlungsverhaltens bei ein-und mehrfacher Kurzzeithärtung bzw, Laserstrahlhärtung des Stahls 42CrMo4, PhD Thesis, Universität Karlsruhe, Shaker, Aachen, 2005, ISBN 3-8322-4689-4.
[23] T. Miokovic′, V. Schulze, O. Vo¨hringer, D. Lo¨he, J. Int, Mater. Prod. Technol. 24 (1–4) (2005) 207–223.
[24] X. Tong, H. Zhou, L. Chen, Z.H. Zhang, L.Q. Ren, Int. J. Fatigue 30 (2008) 1125–1133.
[25] C. Neinhuis, W. Barthlott, Ann. Bot. 79 (6) (1997) 667–677.
[26] T. Kokubo, Thermochim. Acta 280 (1) (1996) 479–490.
[27] T. Kokubo, H.M. Kim, F. Miyaji, H. Takadama, T. Miyazaki, Compos. A: Appl. Sci. Manuf. 30 (44) (1999) 405–409.
[28] L.Q. Ren, Q. Cong, J. Tong, B.C. Chen, J. Terramech. 38 (2001) 211–219.
[29] L.Q. Ren, J.Q. Li, B.C. Chen, Chin. Sci. Bull. 40 (1995) 1077–1080.
[30] L.Q. Ren, J. Tong, J.Q. Li, B.C. Chen, J. Agric. Eng. Res. 79 (2001) 239–263.
[31] H. Zhou, L. Chen, W. Wang, L.Q. Ren, H.Y. Shan, Z.H. Zhang, Mater. Sci. Eng. A 412 (2005) 323–327.
[32] H. Zhou, Y. Cao, Z.H. Zhang, L.Q. Ren, X.Z. Li, Mater. Sci. Eng. A 433 (2006) 144–148.
[33] X. Tong, H. Zhou, Z.H. Zhang, N. Sun, H.Y. Shan, L.Q. Ren, Mater. Sci. Eng. A 467 (2007) 97–103.
[34] H. Zhou, X. Tong, Z.H. Zhang, X.Z. Li, L.Q. Ren, Mater. Sci. Eng. A 428 (2006) 141–147.
[35] H. Zhou, N. Sun, H.Y. Shan, D.Y. Ma, X. Tong, L.Q. Ren, Appl. Surf. Sci. 253 (2007) 9513–9520.
[36] Z.H. Zhang, H. Zhou, L.Q. Ren, X. Tong, H.Y. Shan, Y. Cao, Appl. Surf. Sci. 253 (2007) 8939–8944.
[37] X. Jia, L.Q. Ren, B.C. Chen, Chin. J. Mater. Res. 10 (1996) 556–560.
[38] C. Ion John, Laser Processing of Engineering materials, Elsevier/Butterworth-Heinemann, Oxford, 2005, ISBN: 0-7506-6079-1.
[39] S.P. Lu, H. Fujii, K. Nogi, Mater. Sci. Eng. A 380 (2004) 290–297.
[40] H. Hahn, P. Mondal, K.A. Padmanabhan, Nanostruct. Mater. 9 (1997) 603.